UNCOVERING THE LYSOSOMAL ROLE OF PROGRANULIN

A Thesis

Presented to the Faculty of the Graduate School

of Cornell University

in Partial Fulfillment of the Requirements for the Degree of

Master of Science

By Mitchell Douglas Pagan

May 2019

ABSTRACT

Lysosomes are the degradative centers of the cell and their dysfunction can give rise to lysosomal storage disorders (LSDs). Frontotemporal lobar degeneration (FTLD) is a neurodegenerative disease that exhibits the features of LSDs: the aggregation of proteins in endolysosomal compartments and a decrease in lysosomal activity. One of the genetic causes of FTLD has been traced back to the haploinsufficiency of progranulin (PGRN), a secreted glycoprotein comprised of seven and one-half granulin repeats. PGRN can also be processed into discrete granulin peptides, each with its own potential function. PGRN has been shown to be critical for proper lysosome function, but the mechanism is still unclear. Since PGRN's link to FTLD was established, TMEM106B, a lysosomal transmembrane protein, has been identified as a risk factor for FTLD patients with *GRN* mutations (FTLD-GRN). TMEM106B levels are increased in cases of FTLD-GRN and the overexpression of TMEM106B results in lysosome enlargement and an increase in transcription factor EB-dependent (TFEB) lysosomal exocytosis. TFEB is the transcription factor responsible for the expression of most genes associated with lysosomal biogenesis and its transcriptional activity is increased in ΔGRN cells. Since an increase in TFEB activity is linked to an increase in exocytosis, I hypothesized that the depletion of PGRN results in an increase in lysosomal exocytosis. I assessed whether lysosomal exocytosis is increased in PGRN deficient cells and, while early results showed an increase in exocytosis, further testing generated results that were inconclusive. Proteomic screens to identify binding partners for PGRN and granulin peptides were also carried out, but the procedures need to be optimized. Since this testing was completed, researchers have published data that confirms an increase in lysosomal exocytosis in the absence of *GRN*. This increase in lysosomal exocytosis should be

further characterized by profiling the full spectrum of functional lysosomal enzymes that are excreted into the extracellular space and whether these enzymes negatively impact surrounding neurons. These findings could uncover a mechanistic link between *GRN* mutation, FTLD, and the onset of dementia.

BIOGRAPHICAL SKETCH

Mitchell Pagan was born in Lancaster, Pennsylvania in 1991. After graduating from Manheim Township High School in 2009, Mitchell studied chemistry for a year at Saint Joseph's University before transferring to Ursinus College. He graduated from Ursinus College in 2014 with a Bachelor of Science in biology with a minor concentration in neuroscience. For the next three years Mitchell was employed as a senior chemist in a pharmaceutical product testing role. He then enrolled in the Biochemistry, Molecular and Cell Biology program at Cornell University in the fall of 2017.

ACKNOWLEDGEMENTS

Thank you to my mentor, Dr. Fenghua Hu. The knowledge and experiences I have gained from working in the Hu lab are truly invaluable. Thank you to Dr. Dan Paushter, Dr. Xiaolai Zhou, and Dr. Owen A. Brady for creating the foundation for my work. I'd also like to thank the other members of the Hu lab and the members of the Yuxin Mao lab for their support, constructive criticism, and willingness to troubleshoot experiments. This work was supported by NIH grant R01NS095954 awarded to FH (with Diversity Supplement 02S2 to MDP) and training grant T32GM007273 to MDP.

TABLE OF CONTENTS

LIST OF FIGURES

LIST OF TABLES

LIST OF ABBREVIATIONS

ACN	Acetonitrile
AD	Alzheimer's disease
BAR	Biotinylation by antibody recognition
CathB	Cathepsin B
CathD	Cathepsin D
CathL	Cathepsin L
CLEAR	Coordinated Lysosomal Expression and Regulation
DKO	Double knockout
DMEM	Dulbecco's Modified Eagle Medium
DMSO	Dimethylsulfoxide
DTT	Dithiothreitol
EDTA	Ethylenediaminetetraacetic acid
ER	Endoplasmic reticulum
FBS	Fetal bovine serum
FTLD	Frontotemporal lobar degeneration
GCase	β-glucocerebrosidase
GFP	Green fluorescent protein
GWAS	Genome wide association study
HBSS	Hank's balanced salt solution
HRP	Horseradish peroxidase
IB	Immunoblot
IF	Immunofluorescence
IP	Immunoprecipitation; immunoprecipitate
LC-MS/MS	Liquid chromatography-tandem mass spectrometry
LSD	Lysosomal storage disorder
MEF	Mouse embryonic fibroblast
MPR	Mannose-6-phosphate receptor
NCL	Neuronal ceroid lipofuscinosis
OBB	Odyssey Blocking Buffer
PFA	Paraformaldehyde
PGRN	Progranulin
PSAP	Prosaposin
SDS	Sodium dodecyl sulfate
SILAC	Stable isotope labeling with amino acids in cell culture
SNP	Single nucleotide polymorphism
TBS	Tris-buffered saline
TBST	TBS with 0.1% Tween-20
TCA	Trichloroacetic acid

TDP-43	TAR DNA-binding protein
TFA	Trifluoroacetic acid
TFEB	Transcription factor EB
TMEM106B	Transmembrane protein 106B
UV	Ultraviolet
WB	Western blot
WT	Wild-type

CHAPTER ONE: INTRODUCTION

Lysosomes are the center of degradation and recycling in the cell, harboring a diverse array of enzymes to carry out their function; other lysosomal functions include exocytosis, nutrient sensing, and autophagy [37]. Lysosomal function and cellular degradative capacity are therefore inextricably linked. The absence or dysfunction of lysosomal proteins, whether enzymatic or not, can result in lysosomal storage disorders (LSDs) [37, 47]. LSDs are characterized by a decrease in lysosomal activity and the aggregation of proteins in endolysosomal organelles [37, 47]. One disease that exhibits the typical hallmarks of LSDs is frontotemporal lobar degeneration (FTLD).

FTLD is a neurodegenerative disease and second leading cause of early-onset dementia behind Alzheimer's disease (AD) [50]. It generally manifests as microvacuolation of the brain, nerve cell loss, expansion of ventricles, and atrophy of the frontal and temporal lobes [8, 16, 41, 69]. The severity and prevalence of FTLD has garnered considerable attention from the research community, but the disease mechanism has remained elusive. A lot of the difficulties in studying FTLD arise from the diverse nature of the disease. FTLD can be divided into subgroups based upon the proteins associated with the inclusion bodies. These protein aggregates can be comprised of TAR DNA-binding protein (TDP-43), tau protein, or fused in sarcoma protein [36]. Genetic studies have also revealed that mutations in multiple genes can lead to FTLD. Among the most characterized FTLD-related genes are *GRN*, *MAPT*, and *C9orf72* [49].

Genetic studies, in conjunction with biochemical analyses, uncovered the link between heterozygous mutations in *GRN*, the product of which is progranulin (PGRN), and the onset of FTLD (FTLD-GRN) [14, 18, 36, 39]. Mutations in *GRN* are associated with tau-negative, ubiquitin-positive FTLD, of which TDP-43 is typically aggregated [14, 18, 36, 39]. *GRN*

mutations were found in 10% of the FTLD population and in 23% of familial cases [18]. It was determined that these mutations lead to a haploinsufficiency of PGRN, with most mutations resulting in truncated transcripts [14, 18, 39]. So far, more than 60 mutations in *GRN* have been associated with FTLD [49]. Interestingly, homozygous mutations were later discovered to be the underlying cause of neuronal ceroid lipofuscinosis (NCL), another LSD [2, 56]. FTLD and NCL both display an upregulation of lysosomal proteins, lipofuscinosis, and the accumulation of tau-negative, ubiquitin-positive TDP-43 [19, 30, 68]. This suggested that FTLD could represent a milder form of NCL and that the effects of *GRN* mutations are dose-dependent. It also began to solidify the role of PGRN in the lysosome.

PGRN is a secreted glycoprotein consisting of seven and one-half repeats of a cysteine-rich, β-hairpin stack motif (Figure 1a) [7, 25, 57, 60, 61, 67]. The motifs are connected by short linker regions that are more flexible than the rigid granulins and individual granulin motifs (or peptides) occur naturally [4, 25, 60, 61]. The release of these granulin peptides can occur extracellularly by matrix metalloproteinases and neutrophil elastase or within the lysosome by cathepsin L (CathL) (Figure 1b). PGRN is expressed in epithelial cells, immune cells, and cortical neurons, but very little PGRN is detected in muscle and connective tissue [15]. Its conservation across taxa and expression in unicellular eukaryotes suggests that it has a fundamental role in the cell [45]. While some researchers have implicated PGRN and granulin peptides in processes of growth and inflammation, the function of PGRN has largely remained a mystery [20-23, 34, 35, 40, 48, 55, 71]. It has also been proposed that full-length PGRN and the granulin peptides can act in opposition to one another; some even found that individual granulin peptides have contrasting functions [21-23, 48, 51, 55]. In an attempt to more clearly elucidate the function of PGRN many researchers have now turned their focus to the lysosome.

After its connection to LSDs, PGRN's status as a lysosomal protein has been expanded upon. Predictive models based on protein interactions suggested that PGRN resides in the lysosome and its subcellular residence was confirmed by the colocalization of PGRN with lysosomal markers (e.g. LAMP1, CD68) [6, 26, 40]. PGRN can be trafficked to the lysosome from the trans-Golgi network or from the extracellular space by sortilin, a sorting receptor highly expressed in neurons (Figure 1b) [26, 73]. PGRN can also bind another resident lysosomal protein, prosaposin (PSAP), for trafficking to the lysosome [75-77]. In this instance, PGRN binds PSAP and then PSAP binds a mannose-6-phosphate receptor (MPR) for their subsequent delivery. PSAP can reciprocally hitch a ride with PGRN through the sortilin receptor pathway [76]. Once in the lysosome, PGRN binds cathepsin D (CathD) and aids in its maturation from inactive proCathD to catalytically active matCathD [5, 11, 62]. It has also been shown to act as a co-chaperone that binds β-glucocerebrosidase (GCase), a lysosomal enzyme important in glycolipid metabolism [27]. Loss of PGRN results in the aggregation of GCase and a decrease in its activity (unpublished) [27].

While PGRN's localization, binding partners, and function demonstrate that its primary role exists in the lysosome, its regulation by and of transcription factor EB (TFEB) strengthens this case. TFEB is responsible for the transcription of a majority of the genes necessary for lysosomal biogenesis, also known as the Coordinated Lysosomal Expression and Regulation (CLEAR) network of genes [53]. When overexpressed, TFEB leads to the upregulation of lysosome formation and a rise in degradative capability [53]. Along with these broad effects, the overexpression of TFEB results in a significant increase in PGRN levels [6]. Conversely, when PGRN is overexpressed the lysosomal genes under the control of TFEB are upregulated [6].

While great headway has been made in understanding the lysosomal importance of PGRN, the study of PGRN in relation to FTLD has been complicated. Recapitulating FTLD in mice has proven difficult and *GRN* homozygous mutants do not display an obvious phenotype [1]. However, homozygous *GRN* mutant mice display the phenotypes associated with FTLD: ubiquitin-positive lipofuscin accumulation, hyperphosphorylated TDP-43 inclusions, reduced autophagic flux, behavioral deficits, and decreased life expectancy [1, 12, 70, 72]. Despite the difficulties, additional proteins related to FTLD-GRN have been identified and the big picture, while becoming more complicated, is starting to be revealed.

Transmembrane protein 106B (*TMEM106B*) was identified in a GWAS of FTLD-TDP patients as a risk factor for FTLD-GRN [64]. When compared to FTLD-TDP, FTLD-GRN patients had a higher expression of *TMEM106B* [64]. Researchers also discovered that three *TMEM106B* single nucleotide polymorphisms (SNPs) were able to modulate the penetrance of FTLD-GRN, each with a risk and, less common, protective allele [17, 43, 64, 66]. Only one of the SNPs manifests as a coding variant, T185S [17, 43, 64]. This variant is in linkage disequilibrium with the other SNPs and the expression of the risk allele results in an increase in TMEM106B when compared with the protective allele [13, 17, 43, 64]. Whether the increase in TMEM106B is due to an increase in transcription, a decrease in degradation, or both is disputed [29, 43, 64].

TMEM106B is a type-II transmembrane protein that localizes to endolysosomal compartments [9, 13, 32, 58]. Its entire structure has not been solved, but researchers have determined that its cytosolic N-terminus is intrinsically disordered [28]. Like most lysosomal membrane proteins, TMEM106B's lumenal domain is glycosylated and two of the five sites are crucial for proper sorting into the endolysosomal pathway [32, 58]. While little is known about

its purpose within the cell, researchers have consistently demonstrated abnormal lysosomal phenotypes in the absence and overexpression of TMEM106B. When its expression is upregulated, TMEM106B causes an increase in the size of lysosomes while lysosomes decrease in number; this increase in lysosome size is accompanied by a decrease in degradative capacity [9, 10, 13]. An increase in expression is also associated with the trafficking of lysosomes to the periphery of the cell and an increase in lysosomal exocytosis [31, 54]. The opposite is true when TMEM106B is knocked down, with lysosomes decreasing in size and clustering in the perinuclear region [54, 58].

The mechanism by which TMEM106B can alter the morphology and positioning of lysosomes has not been pinned down, but what we do know is that TMEM106B can influence the activity of TFEB. Along with increasing lysosomal biogenesis, upregulation of TFEB also stimulates lysosomal exocytosis [38]. Scientists have shown that the overexpression of TMEM106B causes the translocation of TFEB from the cytoplasm to the nucleus, an upregulation in lysosomal genes, and an increase in lysosomal exocytosis [31, 58]. The knockdown of TFEB is able to rescue these lysosomal phenotypes when TMEM106B is overexpressed [31]. While much work is still needed to identify TMEM106B's exact function, it undoubtedly plays a role in the lysosome.

Since, the loss of *GRN* increases the activity of TFEB and the overexpression of TMEM106B results in an increase in TFEB-dependent lysosomal exocytosis, I hypothesized that lysosomal exocytosis is increased in Δ*GRN* cells [13, 31, 43, 59, 64]. I assessed lysosomal exocytosis by observing the translocation of TFEB to the nucleus, the deposition of lysosomal markers on the plasma membrane, and the release of lysosomal enzymes into the extracellular space. While early experiments revealed that lysosomal exocytosis was indeed increased in

Δ*GRN* cells, the results became inconclusive after revisiting many of the assays. To open up other avenues of research, I also pursued potential interacting proteins for PGRN and individual granulin peptides through stable isotope labeling with amino acids in cell culture (SILAC) and biotinylation by antibody recognition (BAR) techniques. While the SILAC experiments have not returned any additional hits, I believe that the BAR technique can be optimized and successfully used in the future. Since, completing these preliminary experiments, researchers have documented an increase in lysosomal exocytosis in Δ*GRN* cells [42]. If this increase in lysosomal exocytosis in Δ*GRN* cells is real, the lysosomal enzymes that are expelled into the extracellular space should be characterized and assessed for activity. The release of functional enzymes into the extracellular space could have detrimental effects on neighboring cells and could provide a link between PGRN haploinsufficiency and FTLD.

CHAPTER TWO: RESULTS

Loss of *GRN* may induce an increase in lysosomal exocytosis

It has been established that TMEM106B overexpression leads to the translocation of TFEB to the nucleus, an increase in lysosomal biogenesis, and the induction of lysosomal exocytosis [31, 58]. Researchers have also shown that this increase in lysosomal exocytosis is dependent on TFEB [31]. *TMEM106B* is a modulator of FTLD-GRN penetrance, with higher expression correlated with greater TDP-43 accumulation [43, 63, 64]. Therefore, it stands to reason that general lysosomal dysfunction in concert with higher levels of TMEM106B could lead to lysosomal exocytosis in the case of FTLD-GRN.

To assess lysosomal exocytosis in a Δ*GRN* background, I used Δ*GRN* RAW cells, a murine macrophage line, that our lab had previously generated. Since the documented increases in lysosomal exocytosis were driven by TFEB, I first assessed whether TFEB localization changed in Δ*GRN* cells. At first, it was clear that control cells had a cytosolic distribution of TFEB, with little evidence of translocation of TFEB to the nucleus (Figure 2a). On the other hand, the majority of Δ*GRN* cells had a strong TFEB signal that colocalized with the nucleus. Very few Δ*GRN* cells showed the same cytosolic distribution of TFEB that was seen in the control cells. However, as trials were repeated, more of the control cells began to show a nuclear localization of TFEB (Figure 2b).

While some documented increases in lysosomal exocytosis are dependent upon TFEB, the translocation of TFEB to the nucleus does not demonstrate that lysosomes are fusing with the plasma membrane and expelling their contents into the extracellular space. To assess lysosomal fusion with the plasma membrane, we observed the deposition of LAMP1, a lysosomal marker,

on the plasma membrane. If exocytosis is increased, an increase of surface LAMP1 staining should observed. Compared to control cells, Δ*GRN* cells show an increase in LAMP1 signal on the plasma membrane (Figure 3a). Again, as time went on and experiments were repeated, this difference became negligible, with control cells showing a similar distribution of LAMP1 to Δ*GRN* cells (Figure 3b).

An increase in LAMP1 at the plasma membrane could represent an increase in lysosomal exocytosis, but this does not rule out a trafficking or endocytic defect. We decided that a more definitive measure of exocytosis would be to measure lysosomal proteins in the extracellular space. If exocytosis is increased, lysosomal proteins should be more abundant in the conditioned media of Δ*GRN* cells. Cathepsins, a major class of lysosomal proteases, were slightly increased in the lysates of Δ*GRN* cells, consistent with the documented upregulation of lysosomal genes in the absence of *GRN* (Figure 4). Interestingly, cathepsins were also increased in the conditioned media of Δ*GRN* cells. It is worth noting that the most of the cathepsins in the extracellular space are present in their unprocessed, pro-form.

The identification of binding partners for full-length progranulin and granulin peptides

Scientists have proposed functions for a few granulin peptides, but the binding partners and precise role of each granulin is largely unknown [4, 48, 55, 60]. Pulling down and detecting granulin peptides has been an issue in the past, but our lab has optimized conditions so that immunoprecipitation (IP) of the peptides is feasible. To identify novel interactions between progranulin or granulin peptides, we performed SILAC and BAR experiments.

Granulin constructs

At first, we thought it would be beneficial to create GFP-tagged granulin peptides to individually transfect into Δ*GRN* cells, so that the subsequent IP would result in binding partners specific to each granulin peptide (Table 1). The cloning of each granulin construct was successful and the expression of each peptides was detectable in cell lysates and conditioned media (Figure 5). However, when transfected into cells, the granulin peptides showed an erratic distribution. Some peptides were completely cytosolic and others formed large aggregates (data not shown). Some peptides even showed a mix between diffuse and aggregated signal that differed from cell to cell. More importantly, the colocalization of granulin peptides with lysosomal markers was minimal. In light of these results, we decided to assess the binding partners of endogenous PGRN and granulin peptides.

SILAC of PGRN and granulin peptides

Sheep anti-PGRN beads were created and shown to be specific and capable of pulling down full-length PGRN and granulin peptides (data not shown). Control and Δ*GRN* RAW cells were grown in carbon-13 heavy and carbon-12 light media, respectively. The IP of PGRN was efficient for the cell lysate, but the beads failed to IP PGRN or granulin peptides in the conditioned media (Figure 6). The silver stain of the lysates showed that the IP was relatively clean, so the samples were prepared for and analyzed by liquid chromatography-tandem mass spectrometry (LC-MS/MS). Due to contaminants and lack of granulin peptides in the acquired data set, no conclusions could be drawn (data not shown).

Lysosomal isolation for the enrichment of granulin peptide interactors

PGRN undergoes cleavage events in the lysosome that release individual granulin peptides, so we thought it would be useful to enrich for granulin peptides prior to the identification of interactors [24, 33, 74]. Since granulin peptides should not be present in other

intracellular compartments, identified proteins should be more likely to bind granulin peptides and not full-length PGRN than if whole cell lysate was used.

Before the technique was used for the identification of binding proteins, I first set out to optimize the conditions of lysosomal isolation with wild-type (WT) mouse liver samples. Following the manufacturer's protocol resulted in fairly distinct layers, but there appeared to be an abundance of endoplasmic reticulum (ER) contamination. Gradients have been optimized for different tissue and cell types, so a modified gradient based on the literature was assessed for recovery and elimination of contaminants (Figure 7a) [44, 52]. While the recovery was unaffected, the modified gradient seemed to produce more distinct bands and the ER contamination was slightly reduced (Figures 7b and 7c). Further optimization will be necessary for any proteomic or quantitative analyses.

Identification of PGRN and granulin peptides binding partners through BAR

In conjunction with the SILAC analyses, I attempted to identify potential PGRN interactions through the use of the BAR technique as previously described [3]. For the identification of binding proteins, horseradish peroxidase (HRP) is targeted to the protein of interest with antibodies. Biotin is then added to the reaction, so that HRP can link biotin to proteins in the vicinity of the protein of interest. These surrounding proteins can then be pulled down with streptavidin. Identified proteins do not necessarily bind the protein of interest and any hits would have to be confirmed with additional analyses, but this method could be useful in identifying interactions that may be more transient.

Before the application of this method, I set out to optimize the conditions so that labeling was sufficient and specific. I used the labeling of PGRN-interacting proteins in control and Δ*GRN* mouse embryonic fibroblasts (MEFs) for these purposes. Proteins that interact with

PGRN should be endolysosomal. The staining of biotin after labeling was strong, colocalized with lysosomes, and the signal was dependent on labeling time (Figure 8a). Little to no signal was observed in the Δ*GRN* condition. Since the labeling was deemed specific, I attempted to pull down the labeled proteins with streptavidin. The pulldown of proteins was relatively specific, with the control sample pulling down PSAP, a PGRN-binding protein, more readily than the Δ*GRN* condition (Figure 8b). However, the efficiency of this labeling was much lower than had been observed in the staining. Again, further optimization of this technique will be required before it is used in the identification of interactors.

CHAPTER THREE: DISCUSSION

Loss of *GRN* may induce an increase in lysosomal exocytosis

Characterizing the hallmarks of lysosomal exocytosis in Δ*GRN* cells resulted in some mixed outcomes. The translocation of TFEB to the nucleus and an increase in surface LAMP1 were observed in Δ*GRN* cells in preliminary experiments, but these phenotypes became more inconclusive with time. Of course, the earlier phenotypes could have been a fluke and the repetition of experiments may have revealed a truer depiction of the difference between control and Δ*GRN* cells. However, other analysts and I noticed that these particular macrophages had become quite unhealthy and typically displayed an active, spread out morphology. We would expect to observe an increase in lysosomal biogenesis in these active macrophages. If both the control and Δ*GRN* cells were in their active states and lysosomal biogenesis genes were upregulated, observing a difference between the two conditions would become quite challenging. Indeed, the disappearance of the contrast between control and Δ*GRN* phenotypes closely coincided with our observations that the cells had become stressed.

Lysosomal exocytosis was also assessed by probing for lysosomal enzymes in the conditioned media of control and Δ*GRN* cells. The levels of cathepsins in the conditioned media were consistently higher for Δ*GRN* cells. One would expect to find this increase in lysosomal proteins in the extracellular space if lysosomal exocytosis is upregulated. However, if the origin of these cathepsins is lysosomal, they should be in their mature form. The cathepsins in the conditioned media of both control and Δ*GRN* cells were in their unprocessed, inactive forms.

Instead of lysosomal exocytosis, the observed difference between the two conditions could arise from a change in the trafficking of the enzymes of interest.

While this work was being completed, a report was published describing an increase in lysosomal exophagy in Δ*GRN* macrophages [42]. Exophagy is a term that describes the breakdown of extracellular components by the enzymes residing in lysosomes. Lysosomes release their contents into the extracellular space, macromolecules are degraded, and the degraded contents are then taken up by the cell. This work mirrors the more convincing phenotypes I observed in Δ*GRN* macrophages. It seems as though an increase of lysosome fusion with the plasma membrane and a release of lysosomal contents into the extracellular space are probable in the absence of PGRN.

This release of lysosomal contents could serve as a disease mechanism for FTLD. An increase in the expulsion of lysosomal contents into the extracellular space could adversely affect neighboring cells. While the enzymes I probed for (i.e. CathB and CathL) were in their inactive forms, that does not account for all proteases or other classes of lysosomal enzymes. It would be interesting to see if an increase in enzymatic activity can be detected in the conditioned media of Δ*GRN* cells and whether this media impacts the health of cultured neurons.

The identification of binding partners for full-length progranulin and granulin peptides

The search for additional interactors for both full-length PGRN and granulin peptides was unfruitful. Data from the SILAC experiment was inconclusive and the BAR protocol was never optimized to the point where a mass spectrometry analysis could be performed. While the pulldown of known PGRN interactors was not very efficient and contained some background noise, I was able to successfully amplify the signal of a target protein for imaging. This protocol

can be used by the lab in the future to increase the signal of proteins with low levels of expression.

The search for proteins that interact with granulin peptides will continue to be arduous. It is clear that the GFP-tagged granulin constructs that I created will be of little use for these purposes. The GFP tag is larger than the individual granulin peptides and most likely affects their function and localization. Creating granulin peptides with a less intrusive tag could reduce the unintended consequences, but their trafficking to the lysosome would still remain an issue. PGRN and granulin E can bind sortilin, but routes for the other granulin peptides to the lysosome, if they exist, are unknown [26, 73]. Granulins should not bind many proteins in the cell outside of the lysosome, so their delivery to this compartment is absolutely necessary. For these reasons, the search for granulin peptide binding partners will most likely have to be completed with endogenous protein.

CHAPTER FOUR: FIGURES

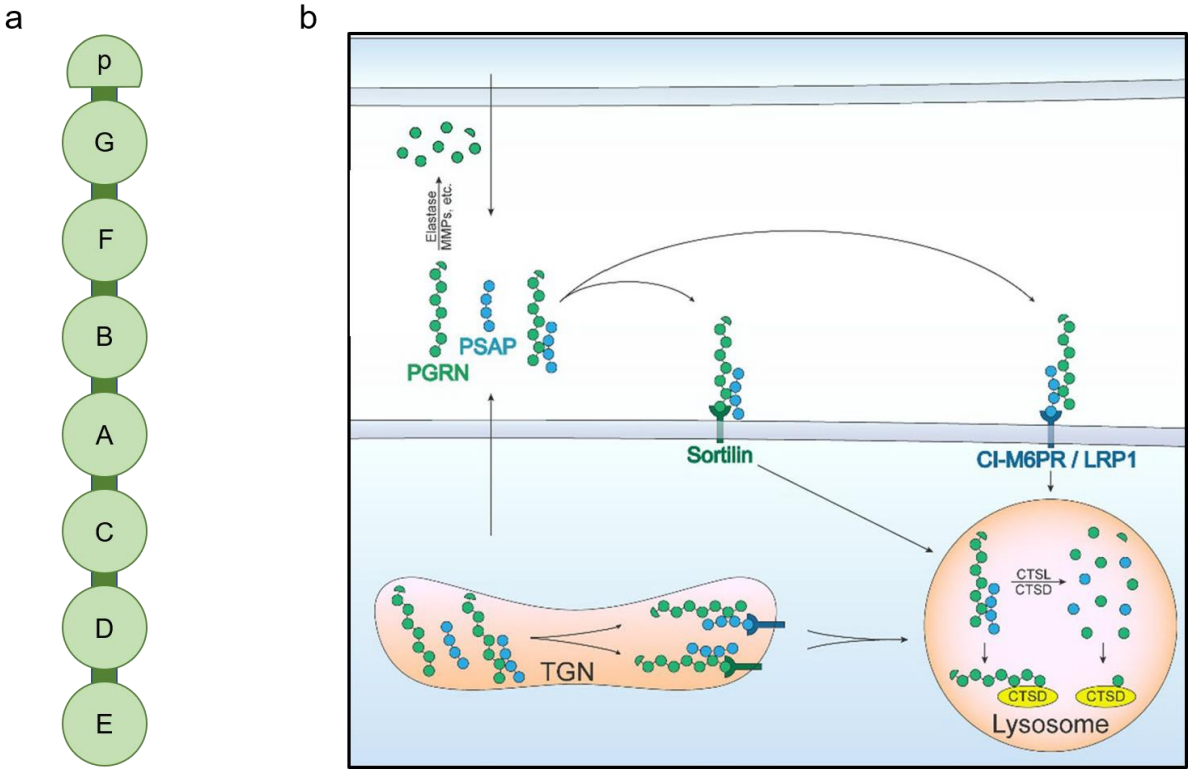

Figure 1: The architecture, trafficking, and processing of progranulin.

(a) A representation of PGRN with its seven and one-half granulin repeats. The short linker regions are depicted in dark green. (b) A schematic of the trafficking of PGRN by sortilin and co-trafficking with PSAP. The cleavage of PGRN is shown in the extracellular space and lysosome with the respective proteases. This figure was adapted from Daniel Paushter [46].

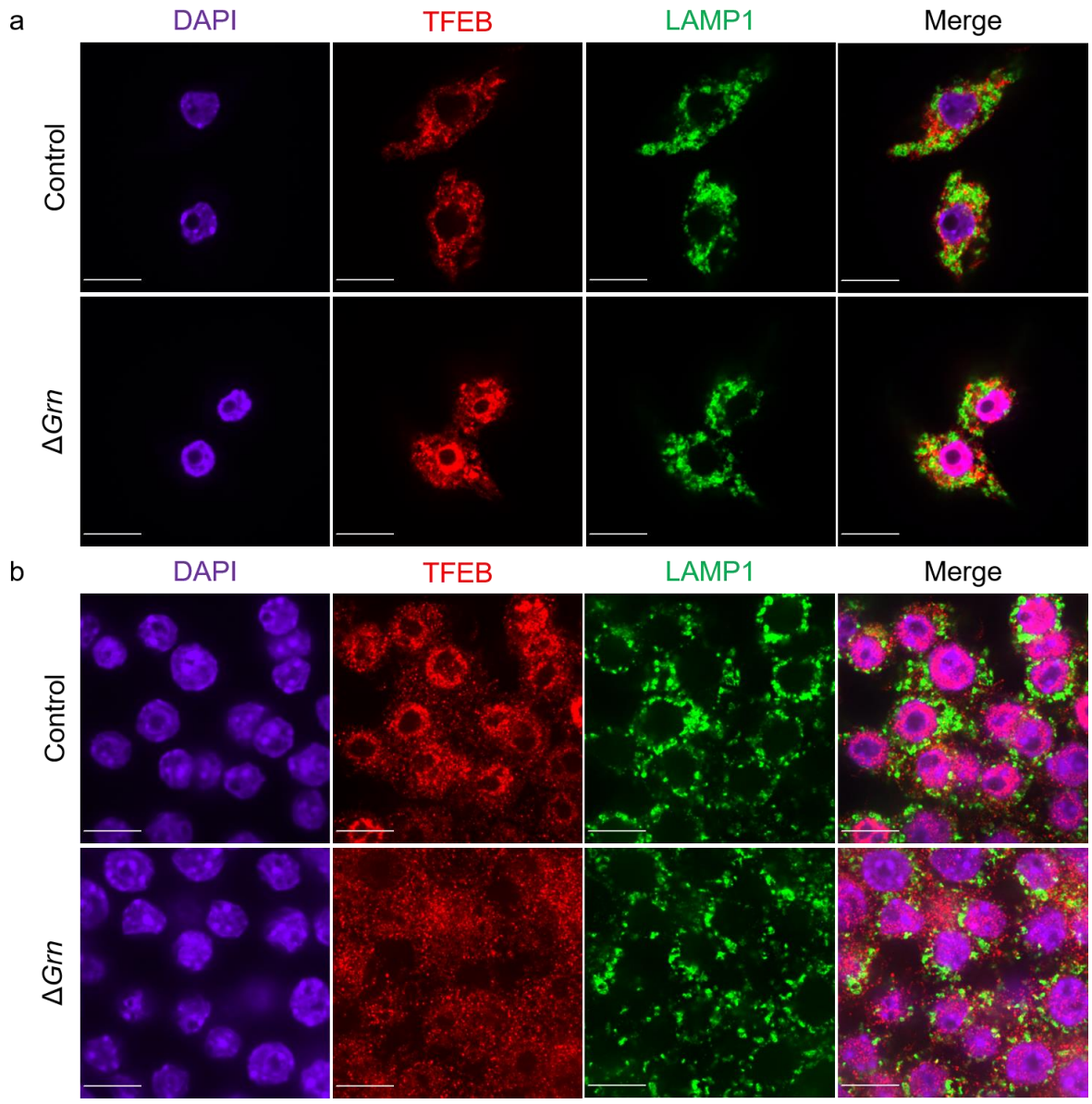

Figure 2: **Localization of TFEB in Δ*GRN* RAW cells.**

Control and Δ*GRN* RAW cells were fixed and stained with anti-TFEB and anti-LAMP1 antibodies, along with DAPI. (a) A representative set of images from earlier experiments shows that TFEB is more localized to the nucleus in Δ*GRN* cells when compared to controls. (b) A representative set of images from later experiments showing the loss of this difference between control and Δ*GRN* cells. Scale bars: 10µm.

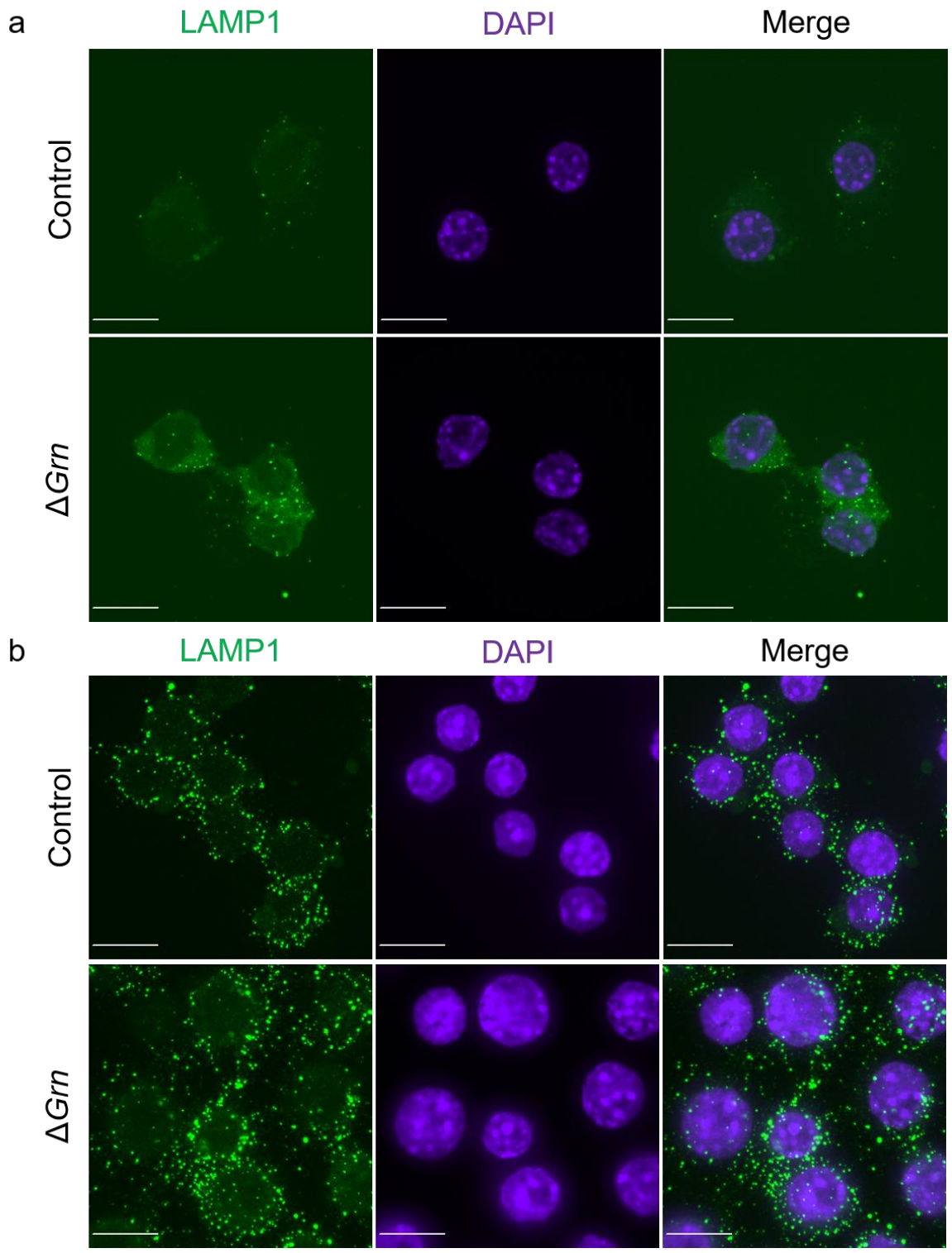
a
LAMP1
DAPI
Merge
Control
ΔGrn
b
LAMP1
DAPI
Merge
Control
ΔGrn

Figure 3: Surface LAMP1 staining in Δ*GRN* RAW cells.

To assess lysosomal exocytosis, live-staining of surface LAMP1 was performed on control and Δ*GRN* RAW cells. To avoid permeabilization and labeling of internal LAMP1, cells were incubated on ice with anti-LAMP1 antibody in 1X HBSS with 20mM HEPES for 2 hours. Cells were then fixed and stained with secondary antibody. (a) Representative images from earlier experiments that show an evident increase in surface LAMP1 staining in Δ*GRN* cells. (b) Images from later experiments showing a decrease in the difference in surface LAMP1 staining between control and Δ*GRN* cells. Scale bars: 10µm.

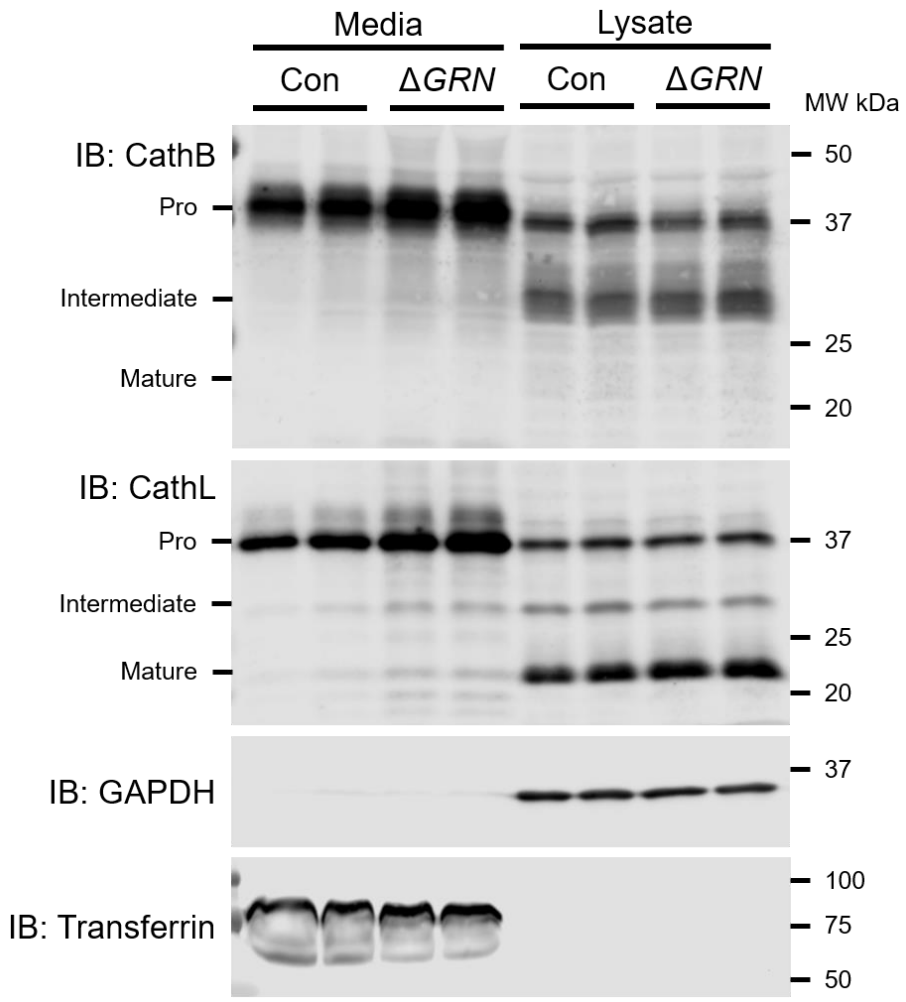

Figure 4: Cathepsins are increased in the conditioned media of Δ*GRN* RAW cells.

The lysates and conditioned media of control and Δ*GRN* cells were probed for cathepsins with anti-CathB and anti-CathL antibodies. CathL, and to a lesser extent, CathB are increased in the conditioned media of Δ*GRN* cells. The majority of both cathepsins in the media are present in their pro-forms. GAPDH and transferrin were immunoblotted as lysate and media controls, respectively.

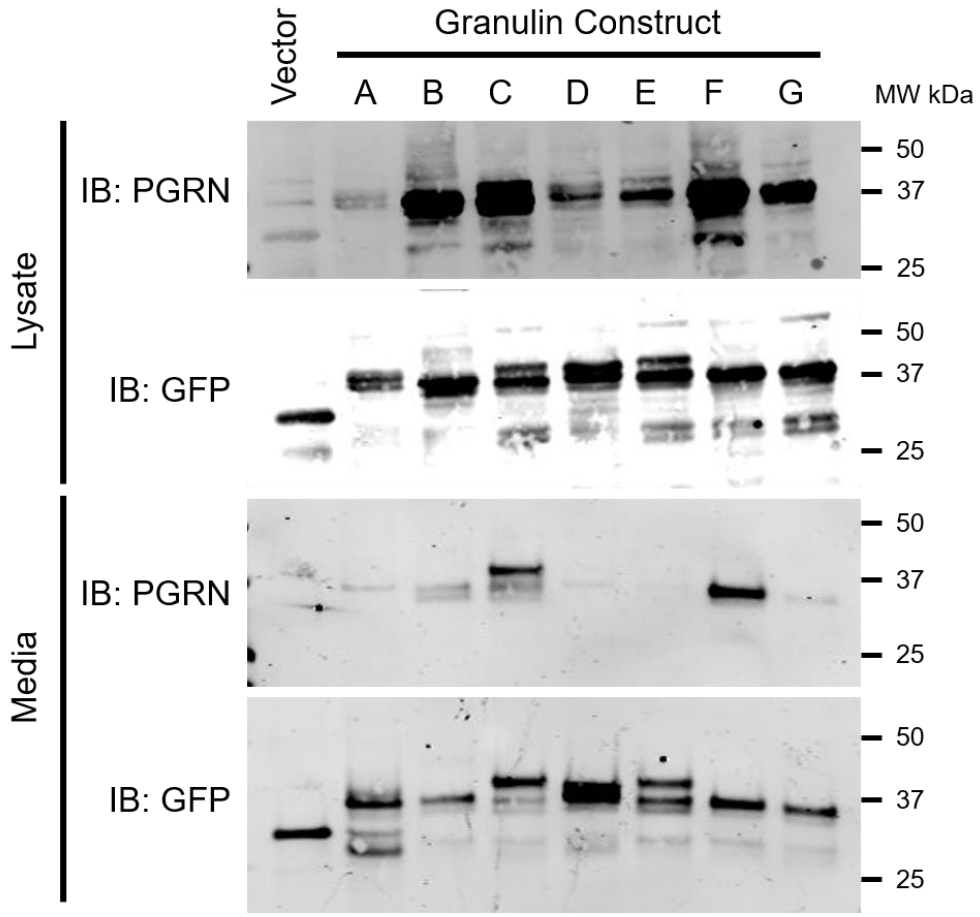

Figure 5: **The expression of granulin peptides in HEK293T cells.**

GFP-tagged granulin peptides were individually transfected into HEK293T cells to evaluate their expression. Each of the granulin peptides was detected in the lysate and media. The anti-PGRN antibody was able to detect all of the granulin peptides, but to a lesser extent in the conditioned media.

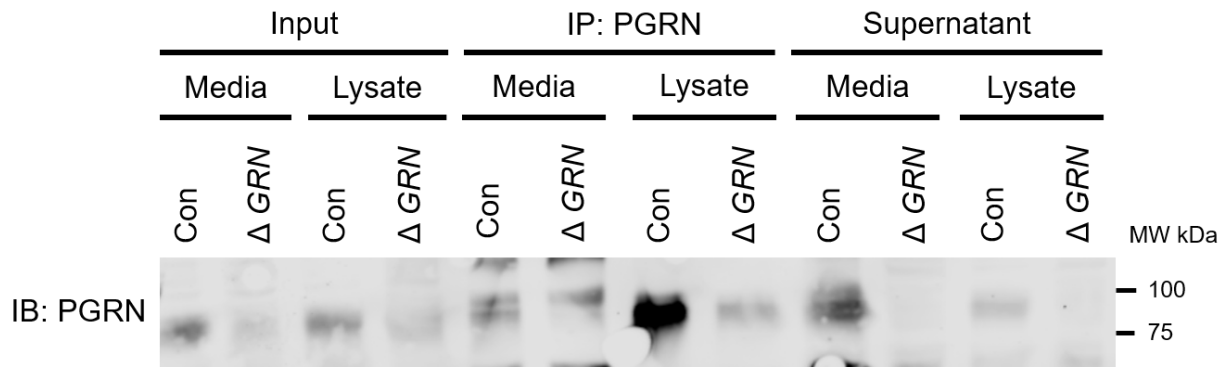

Figure 6: **Western blot confirmation for the SILAC of PGRN and granulin peptides.** Control and Δ*GRN* cells were grown in carbon-13 heavy and carbon-12 light media, respectively. Anti-PGRN beads were used to IP PGRN in the lysates and conditioned media of each sample. PGRN was pulled down in the lysate, but very little PGRN was observed in the media; therefore, only the lysate samples were prepared for LC-MS/MS

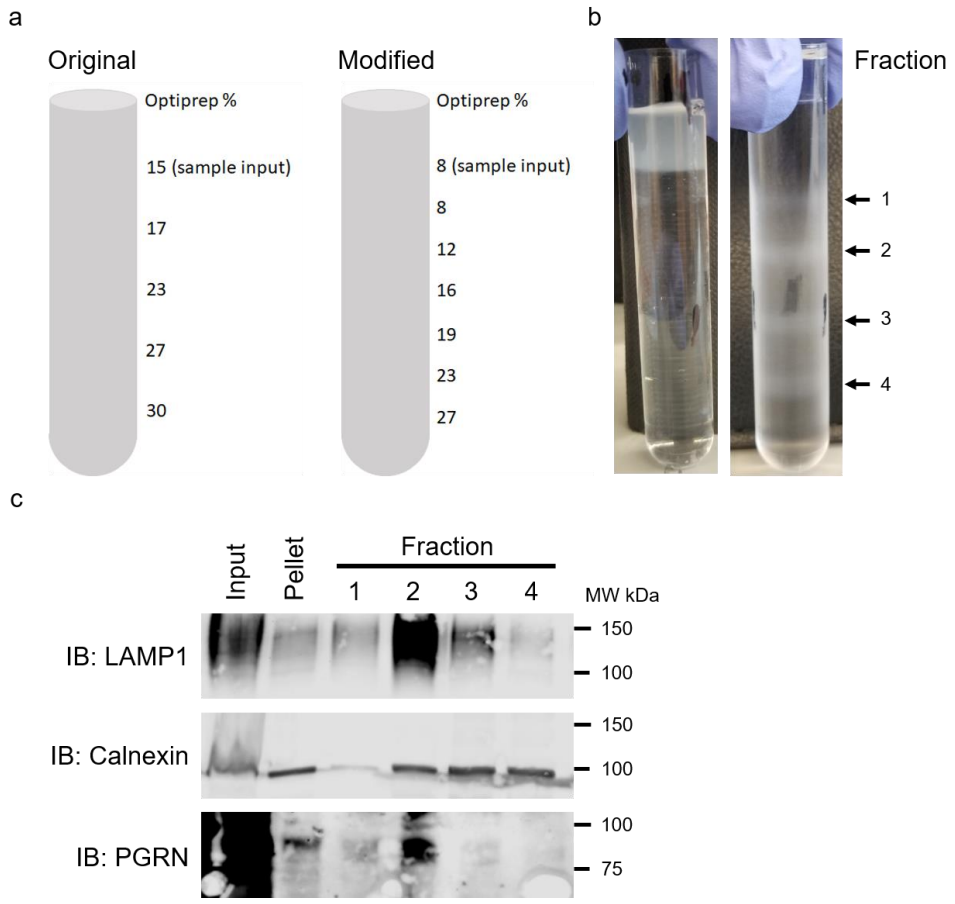

Figure 7: **Optimization of lysosome isolation for potential downstream processing.** Lysosome isolation was completed as per the manufacturer's protocol with a modified gradient using WT mouse liver. (a) Representation of the original, manufacturer-suggested gradient and the modified gradient adapted from the literature [44, 52]. (b) A representative sample using the modified gradient pre- (left) and post-centrifugation (right). (c) A Western blot showing that LAMP1, a lysosomal marker, was enriched in fraction 2. IB of calnexin was used to determine the amount of ER contamination. "Pellet" samples originate from the very first centrifugation step and should contain only whole cells and denser organelles.

a

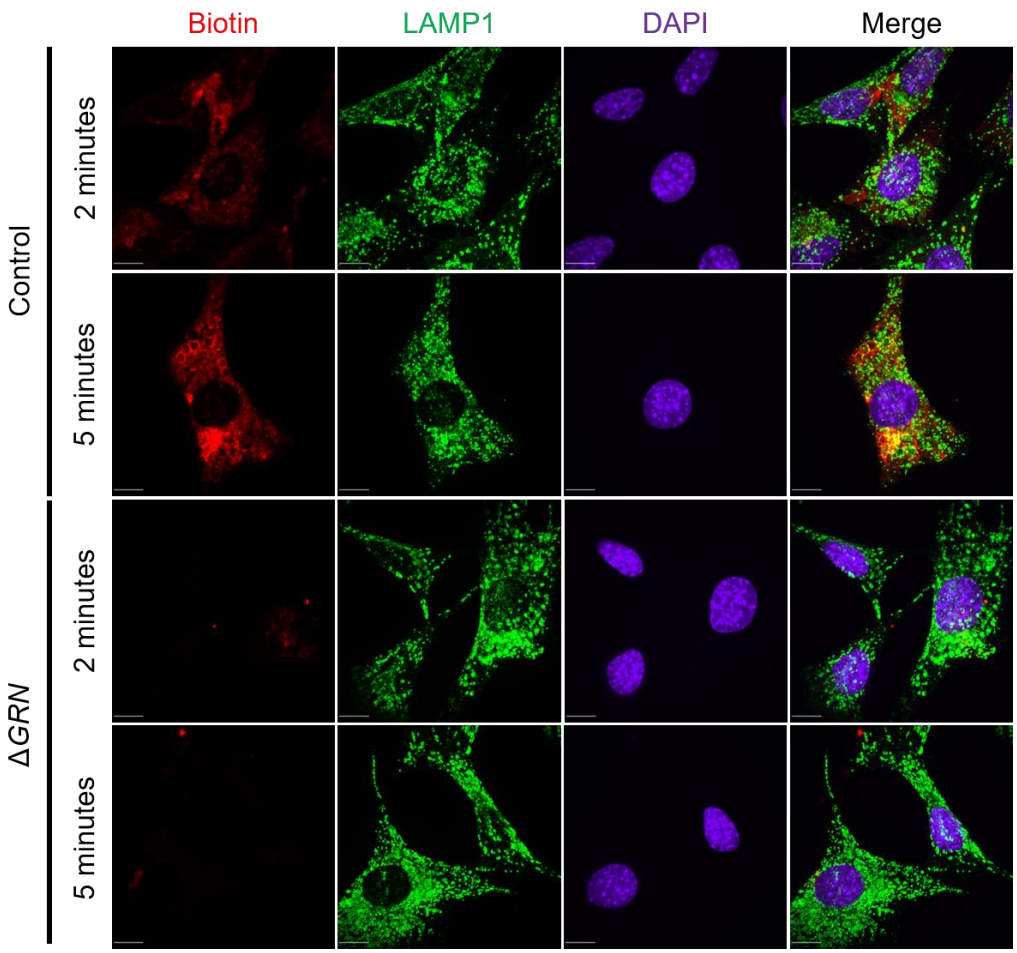
Biotin
LAMP1
DAPI
Merge
Control
2 minutes
5 minutes
ΔGRN
2 minutes
5 minutes

b

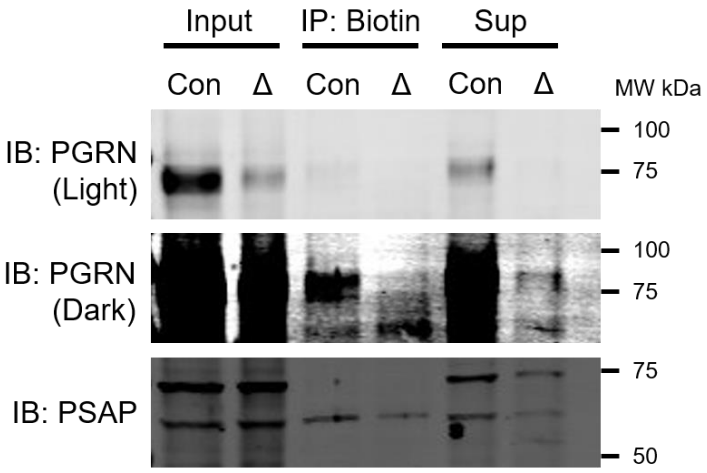
Input
IP: Biotin
Sup
Con
Δ
Con
Δ
Con
Δ
MW kDa
IB: PGRN (Light)
100
75
IB: PGRN (Dark)
100
75
IB: PSAP
75
50

Figure 8: BAR protocol optimization and assessment via microscopy and western blot. To evaluate the specificity and degree of labeling, PGRN was used as a target protein in control and Δ*GRN* MEF cells. (a) The BAR analysis was completed as per the manufacturer's protocol and then stained for biotin and LAMP1. Since PGRN was used as the target protein, colocalization of biotin and LAMP1 should be observed. The labeling of samples was specific and time-dependent, with labeling for 5 minutes greatly increasing the signal when compared with samples labeled for 2 minutes. Little to no labeling was observed in the Δ*GRN* MEFs. Scale bars: 10μm. (b) The streptavidin enrichment for biotinylated proteins after labeling as previously described, with PGRN as a target protein [3]. If the labeling and pulldown were efficient, PGRN and PSAP, a known PGRN interactor, should be observed in the IB. PGRN and PSAP were present, but at very low levels. The labeling of PSAP was also only slightly higher in the control compared to the Δ*GRN* condition. Sup = supernatant.

Granulin Peptide	Sequence of Amino Acids
GrnA	DVKCDMEVSCPDGYTCCRLQSGAWGCCPFTQAVCCEDHIHCCPAGFTCDTQKGTCEQGPHQVPWMEKAPAHLSLPDPQALKR
GrnB	SVMCPDARSRCPDGSTCCELPSGKYGCCPMPNATCCSDHLHCCPQDTVCDLIQSKCLSKENATTDLLTKLPAHTVG
GrnC	DVPCDNVSSCPSSDTCCQLTSGEWGCCPIPEAVCCSDHQHCCPQGYTCVAEGQCQRGSEIVAGLEKMPARRASLSHPR
GrnD	DIGCDQHTSCPVGQTCCPSLGGSWACCQLPHAVCCEDRQHCCPAGYTCNVKARSCEKEVVSAQPATFLARSPHVGVK
GrnE	DVECGEGHFCHDNQTCCRDNRQGWACCPYRQGVCCADRRHCCPAGFRCAARGTKCLRREAPRWDAPLRDPALRQLL
GrnF	AIQCPDSQFECPDFSTCCVMVDGSWGCCPMPQASCCEDRVHCCPHGAFCDLVHTRCITPTGTHPLAKKLPAQRTNRAVALSS
GrnG	GGPCQVDAHCSAGHSCIFTVSGTSSCCPFPEAVACGDGHHCCPRGFHCSADGRSCFQRSGNNSVG

Table 1: Granulin peptide constructs.

The amino acid sequence for each granulin peptide. The constructs we created include the underlined amino acids. All granulin peptide constructs are tagged with GFP at the N-terminus. The amino acids that are not underlined represent the linker regions between granulin peptides. Documented cleavage sites are delineated by the amino acids in red [33].

CHAPTER FIVE: EXPERIMENTAL PROCEDURES

Cell Culture

HEK293T and MEF cells were grown in Dulbecco's Modified Eagle Medium (DMEM) (Corning Cellgro) with 10% FBS; RAW cells were grown in DMEM with 10% FBS and 3µg/ml puromycin. All cells were kept at 37°C with 5% CO_2. Transfections were carried out as described [65].

Plasmids

Mouse PGRN cDNA was obtained from Sino Biological, Inc. Granulin constructs were cloned into PCDH-Puro vectors (System Biosciences) in a three-way ligation with GFP using restriction enzymes NheI, BamHI-HF, PmeI, and SwaI (New England Biolabs, Inc.).

Antibodies and Chemicals

Antibodies and their dilutions used are as follows: rabbit anti-TFEB (Proteintech 13372-1-AP; IF 1:200), mouse anti-GAPDH (Proteintech 60004-1-Ig; WB 1:5000), goat anti-CathB (R&D Systems AF965; WB 1:500), goat anti-CathL (R&D Systems AF1515; WB 1:500), rabbit anti-transferrin (Proteintech 17435-1-AP; WB 1:1000), sheep anti-mouse PGRN (R&D Systems AF2557; WB 1:1000), rabbit anti-calnexin (Abcam ab22595; WB 1:3000), and rabbit anti-GFP (homemade B79D; WB 1:5000). The rabbit anti-mouse PSAP antibody used has been previously described (WB: 1:1,000) [76]. The hoechst (referred to as DAPI throughout the text) used for nuclear staining was homemade (IF 1:2000). Streptavidin 549 (Vector Labs SA-5549; IF 1:500) was used for the detection of biotin in the staining of BAR samples.

Immunofluorescence Microscopy

Transfections were performed two days prior to fixation. For assays not requiring transfection, cells were added to glass coverslips the day before fixation. Cells were washed twice with cold phosphate-buffered saline (PBS) and then fixed in 4% paraformaldehyde (PFA) for 15-20 minutes. Cells were then rinsed three times with PBS. Permeabilization of cells was performed with 0.05% saponin in Odyssey Blocking Buffer (LI-COR Biosciences) (OBB) for 30 minutes. Primary antibodies in OBB with 0.05% saponin were applied to the cells overnight at 4°C. The following day, cells were rinsed with 0.05% saponin in PBS three time for ten minutes. Secondary antibodies in OBB with 0.05% saponin were applied to the cells for in the dark for two hours at room temperature. They were then rinsed with 0.05% saponin in PBS three times for ten minutes. Coverslips were mounted onto slides with Fluromount-G (Southern Biotech). Confocal images were acquired with a ZEISS LSM 700 confocal microscope with a 100x objective. Images were analyzed with SlideBook 6 (3i – Intelligent Imaging Innovations) software.

Live-Cell Staining

While on ice, the media was removed and the cells were rinsed twice with cold PBS. 1X Hanks' balanced salt solution (HBSS) with 20mM HEPES containing primary antibodies was added to the cells and incubated on ice for 2 hours. Cells were then rinsed twice with cold 1X HBSS with 20mM HEPES and then fixed with cold 4% PFA for 15-20 minutes. Cells were then rinsed three times with PBS. Cells were blocked in OBB (with or without 0.05% saponin) for 30 minutes. Secondary antibodies in OBB (with or without 0.05% saponin) were applied to the cells

for 2 hours at room temperature in the dark. Coverslips were rinsed three time with PBS and then mounted onto slides with Fluoromount-G.

Trichloroacetic Acid (TCA) Precipitation of Conditioned Media

First, 900µl of conditioned media was collected and centrifuged for 10 minutes at 14000rpm at 4°C. The supernatant (~900µl) was collected and transferred to a new tube. Then, 100µl of 100% TCA was added. Samples were incubated on ice for 30 minutes and then centrifuged for 20 minutes at 14000rpm at 4°C. The supernatant was discarded. The pellet was washed with 1-1.5ml cold acetone and vortexed. Samples were then centrifuged for 15 minutes at 14000rpm at 4°C. The supernatant was discarded and the pellet was airdried for 10-20 minutes. 30µl of 2x SDS loading buffer was added to the samples and pipetted up and down to resuspend the pellet. If the solution was yellow (low pH), 1µl of 1M Tris pH 8.8 was added. Samples were vortexed well.

SILAC Immunoprecipitation and Sample Preparation

Immunoprecipitation

Control and Δ*GRN* RAW cells were grown in carbon-13 heavy and carbon-12 light media, respectively, for at least seven passages. Cells were cultured in 15cm dishes. The media was aspirated off of the dishes and the cells were washed three times with cold PBS. 1-2ml of IP lysis buffer (50mM Tris-HCl, 150mM NaCl, 1% Triton, 0.1% sodium deoxycholate, and protease inhibitors) were added to the dishes. Cells were scraped from the dishes and the lysates were collected in 2ml Eppendorf tubes. Samples were centrifuged for 20 minutes at 14000rpm at 4°C. The supernatants were transferred to new tubes and 20µl was saved as input. 20µl of sheep

anti-PGRN beads were added to the samples and rocked at 4°C for 4 hours. The beads were centrifuged at 3000rpm for 1 minute at 4°C. 20µl of the supernatants were saved. The remainder of the supernatant was aspirated off and the beads were washed four times with IP wash buffer (50mM Tris-HCl, 150mM NaCl, 1% Triton), spinning down beads at 6000rpm for 30 seconds at 4°C. After removing as much supernatant as possible, 40µl of elution buffer (1% SDS, 100mM Tris pH 8.0) were added to the samples. They were then boiled for 5 minutes and the beads were transferred to a filter tube. The filter tubes were spun down at 10000rpm for 1 minute. Another 40µl of elution buffer were added to the tube originally containing the beads to ensure all beads were captured. The solution was then transferred to the filter tube and spun down once again at 10000rpm for 1 minute. Samples were then analyzed by silver stain and Western blot.

Sample Preparation

DTT was diluted to a final concentration of 10mM in the eluted sample and incubated at room temperature for 15 minutes. A 20X iodoacetamide solution (0.5M in 1M Tris pH 8.0) was diluted down to 1X in the samples. The heavy and light solutions were then mixed. Proteins were precipitated by adding three sample volumes of PPT solution (50% acetone, 49.9% ethanol, 0.1% acetic acid) and incubating on ice for 30 minutes. Samples were centrifuged at 14000rpm for 10 minutes at 4°C. The supernatant was discarded and the pellet was washed with 200µl of PPT solution. Samples were sonicated in a water bath for 30 seconds. Samples were then centrifuged at 14000rpm for 10 minutes at 4°C and the supernatant was discarded. The samples were airdried for 5 minutes. Pellets were resuspended in 50µl of Urea/Tris (8M Urea, 50mM Tris pH 8.0) and then 150µl of NaCl/Tris (50mM Tris pH 8.0, 150mM NaCl). 1µg of trypsin gold (Promega) was added to each sample and digested overnight on a nutator set to 37°C.

The next day, 5µl of 10% TFA and 5µl of 10% formic acid were added to the samples using a glass syringe. The pH was checked to ensure it was ~2. A Sep-Pak C18 column (Waters WAT054955) was conditioned with 1ml of 80% ACN and 0.1% acetic acid. The column was then equilibrated with 1 ml of 0.1% TFA. The sample was loaded and run through the column. The column was then washed twice with 1ml of 0.1% acetic acid, rinsing the syringe between the two additions. Samples were eluted into silanized vials with 200µl of 80% ACN and 0.1% acetic acid. Samples were mixed by pipetting up and down. 20µl of the sample were transferred to another silanized vial. Both silanized vials were dried for 40 minutes at 45°C. The 10% sample was resuspended in 7µl of 0.1P (0.1pmol angiotensin). 15µl of ddH_2O was added to the 90% sample and it was frozen at -80°C. Samples were analyzed by Shannon Marshall of the Marcus Smolka lab.

Western Blot Analysis

Cells were rinsed three times with cold PBS and then collected in RIPA buffer (1% Triton, 0.5% deoxycholate, 0.1% SDS, 150mM NaCl, 150mM Tris HCl pH 8.0, protease inhibitor; 100µl for a 6-well dish). Samples were sonicated and combined with 2x Laemmli buffer with 5% β-mercaptoethanol. Samples were heated at 95°C for five minutes before being loaded into a 12% SDS-PAGE gel. Samples were transferred to Immobilon-FL membranes (Millipore IPFL00010). Membranes were blocked for 1 hour in 5% nonfat dry milk in PBS or OBB. Membranes were then rinsed three times with TBS with 0.1% Tween-20 (TBST) for ten minutes. Primary antibodies in TBST were added the membranes and rocked overnight at 4°C. The membranes were rinsed with TBST three times for ten minutes. Secondary antibodies in TBST were then added to the membranes and rocked for 1 hour at room temperature. The

membranes were rinsed with TBST three times for ten minutes. Membranes were scanned on a LI-COR Odyssey CLx.

Lysosomal Isolation

A Thermo Scientific Lysosome Enrichment Kit for Tissue and Cultured Cells (#89839) was used for lysosome purification. There are two general steps in lysosome purification: lysis of cells or tissue and centrifugation/purification of lysosomes. Regardless of cell or tissue preparation, protease inhibitor was added to Reagents A and B just prior to use.

Cultured Cells and Sonication

50-200mg of cells (1-15cm dish ≈ 50mg of cells) were collected in a 2ml Eppendorf tube. Samples were pelleted at ~850 x g for 2 minutes at 4°C and the supernatant was discarded. 800µl of Reagent A were added to the samples. Samples were vortexed for 5 seconds and then incubated on ice for 2 minutes (did not exceed the 2-minute incubation time). Samples were sonicated with a Branson Digital Sonifier 450 with 3 pulses at 10% power. Cell lysis was confirmed by adding 5µl of lysate to a glass slide with 1µl of Trypan Blue and assessing the ratio of free nuclei to intracellular nuclei. A comparison to non-lysed cells can be used if needed. 800µl Reagent B were added to the samples and tubes were inverted several times to mix. They were then centrifuged at 500 x g for 10 minutes at 4°C. The supernatant was collected and transferred to a new tube. Proceeded to density gradient centrifugation and lysosome clean-up.

Soft Tissue and Electric Pestle Homogenization

In a 2ml Eppendorf tube, 50-200 mg (typically 200mg) of tissue were washed twice with 2ml PBS and the PBS wash was discarded. The tissues were minced into small pieces with a razor blade and then 800µl of Reagent A were added to the samples. Homogenization was

performed with a Kimble Cordless Pellet Pestle (#749540-0000). The pestle attachments were rinsed with 70% ethanol and chilled on ice before use. Tissues were homogenized with 5 pulses. The lysis efficiency was then assessed by adding 5µl of lysate to a glass slide with 1µl of Trypan Blue and assessing the ratio of free nuclei to intracellular nuclei. This process was repeated until the lysis was deemed acceptable. 800µl of Reagent B were added and the tubes were inverted several times to mix. Samples were centrifuged at 500 x g for 10 minutes at 4°C. The supernatant was collected and transferred to a new tube. Proceeded to density gradient centrifugation and lysosome clean-up.

Density Gradient Centrifugation and Lysosome Clean-Up

From the stock 60% OptiPrep solution, discontinuous gradients were created by diluting down the OptiPrep in Gradient Dilution Buffer (1:1 Reagent A: Reagent B). Gradients were top-loaded into an ultracentrifuge tube, starting with the highest concentration and working down to the lowest concentration. Gradients used (%OptiPrep): 17, 20, 23, 27, 20 or 8, 12, 16, 19, 23, 27. 1500µl of the prepared sample was then combined with OptiPrep so that it would lay on top of the density gradient (i.e. equal or lower concentration than the lowest gradient density). Samples were then loaded on top of the discontinuous gradient. The ultracentrifuge tubes were filled to the top with light mineral oil. Using a Beckman Coulter L-series ultracentrifuge with an SW 41 Ti swinging-bucket rotor, samples were centrifuged at 141000 x g (SW 41 Ti limit) for 2 hours at 4°C. Each fraction was collected in 1.5ml Eppendorf tubes. Enough room was left in the tubes so that the fractions could be diluted with 2-3 volumes of PBS. This step is crucial and single fractions were split into multiple tubes when collecting more than 500µl. Samples were gently vortexed to mix. Samples were centrifuged at 18000 x g for 30 minutes at 4°C. The supernatant was removed and the lysosome pellet was kept on ice. The pellet was surface-washed with 1ml

of Gradient Dilution Buffer and then centrifuged at 18000 x g for 30 minutes at 4°C. The supernatant was removed and the lysosome pellet was kept on ice for further processing. For these assays, samples were simply combined with 30µl of 2x Laemmli buffer with 5% β-mercaptoethanol and analyzed by WB.

BAR Protocol

For labeling, an Invitrogen Biotin XX Tyramide SuperBoost Kit (#B40921) was used in conjunction with a donkey anti-sheep IgG secondary antibody, HRP (#A16041). Procedures were adapted from the accompanying manual (MAN0015834, Rev. B.0) and literature [3].

Validation Through Cell Staining

Cells on coverslips were rinsed three times with cold PBS, fixed for 15 minutes in cold 4% PFA, and then rinsed three times with PBS. Cells were then permeabilized with 0.05% saponin in PBS for 30 minutes. Endogenous peroxidase activity was quenched by incubating the cells in 3% hydrogen peroxide for 1 hour at room temperature. Cells were rinsed three times with 0.05% saponin in PBS. 0.05% saponin in OBB was added to samples and incubated at room temperature for 1 hour. Primary antibodies (e.g. sheep anti-PGRN) in OBB with 0.05% saponin were added to samples and incubated overnight at 4°C.

The following day, coverslips were rinsed three times with 0.05% saponin in PBS for 10 minutes (30 minutes total). The poly-HRP secondary antibody (1:1000) was added to the cells and incubated at room temperature for 1 hour. Cells were rinsed three times with 0.05% saponin in PBS for 10 minutes (30 minutes total). 100µl of the working tyramide solution was applied to the coverslips for the designated amount of time (e.g. 2 or 5 minutes). The reaction was quenched with 100µl of reaction stop reagent working solution. Cells were rinsed three times with 0.05%

saponin in PBS for 10 minutes (30 minutes total). Secondary antibodies and Streptavidin 549 in OBB with 0.05% saponin were added to coverslips for 2 hours at room temperature. Coverslips were then rinsed three times with 0.05% saponin in PBS for 20 minutes (60 minutes total). Coverslips were then mounted on glass slides with Fluoromount-G.

Validation Through Western Blot

Samples consisted either of cultured cells in 10cm dishes or liver tissue (50mg sections). The centrifugation of cells between solution changes always occurred at 2000rpm for 3 minutes.

Cells were collected in cold 0.5mM EDTA in PBS, spun down, and rinsed twice with cold PBS. Cells and tissues were fixed in cold 4% PFA for 10 minutes and 2 hours, respectively. Samples were then spun down and rinsed three times with PBS. Samples were then permeabilized for 30 minutes with 0.05% saponin in PBS. Endogenous peroxidase activity was quenched with the addition of 3% hydrogen peroxide and subsequent 1-hour incubation. Enough hydrogen peroxide was added to cover the samples. Samples were rinsed three times with 0.05% saponin in PBS. OBB with 0.05% saponin was added to each sample and incubated at room temperature for 1 hour. Primary antibodies in OBB with 0.05% saponin were added to the samples and incubated overnight at 4°C.

The following day, the samples were rinsed three times with 0.05% saponin in PBS for 10 minutes (30 minutes total). The poly-HRP-conjugated secondary antibody (1:1000) was added to the samples and incubated at room temperature for 1 hour. Samples were rinsed three times with 0.05% saponin in PBS for 10 minutes (30 minutes total). 100µl of tyramide working solution (enough to cover the samples) were applied to the samples and incubated for the designated time at room temperature. The reactions were quenched with the addition of 100µl of reaction stop reagent working solution. Samples were rinsed three times with 0.05% saponin in PBS. Sample

volumes were adjusted to 0.1ml PBS and 30µl of 10% SDS were added. Samples were heated for 1 hour at 95°C with mild shaking to dissolve samples completely. Samples were heated for longer if samples had not completely dissolved. The samples were then centrifuged for 5 minutes at 14000rpm. Supernatants were collected in a new Eppendorf tube, adjusted to 1ml with PBS and ~10% of samples were saved as input. 25µl of streptavidin beads were added to the samples and incubated at room temperature for 2 hours with rocking. The beads were spun down at 6000rpm for 30 seconds and ~10% of the supernatant was saved. The beads were washed once with PBS, twice with 1M NaCl in PBS, and twice more with PBS. Samples were then analyzed by WB.

REFERENCES

1 Ahmed, Z. *et al.* Accelerated lipofuscinosis and ubiquitination in granulin knockout mice suggest a role for progranulin in successful aging. *The American journal of pathology* **177**, 311-324 (2010).

2 Almeida, M. R. *et al.* Portuguese family with the co-occurrence of frontotemporal lobar degeneration and neuronal ceroid lipofuscinosis phenotypes due to progranulin gene mutation. *Neurobiology of aging* **41**, 200. e201-200. e205 (2016).

3 Bar, D. Z. *et al.* Biotinylation by antibody recognition—a method for proximity labeling. *Nature methods* **15**, 127 (2018).

4 Bateman, A., Belcourt, D., Bennett, H., Lazure, C. & Solomon, S. Granulins, a novel class of peptide from leukocytes. *Biochemical and biophysical research communications* **173**, 1161-1168 (1990).

5 Beel, S. *et al.* Progranulin functions as a cathepsin D chaperone to stimulate axonal outgrowth in vivo. *Human molecular genetics* **26**, 2850-2863 (2017).

6 Belcastro, V. *et al.* Transcriptional gene network inference from a massive dataset elucidates transcriptome organization and gene function. *Nucleic acids research* **39**, 8677-8688 (2011).

7 Bhandari, V., Palfree, R. & Bateman, A. Isolation and sequence of the granulin precursor cDNA from human bone marrow reveals tandem cysteine-rich granulin domains. *Proceedings of the National Academy of Sciences* **89**, 1715-1719 (1992).

8 Bigio, E. H. Making the diagnosis of frontotemporal lobar degeneration. *Archives of pathology & laboratory medicine* **137**, 314-325 (2013).

9 Brady, O. A., Zheng, Y., Murphy, K., Huang, M. & Hu, F. The frontotemporal lobar degeneration risk factor, TMEM106B, regulates lysosomal morphology and function. *Human molecular genetics* **22**, 685-695 (2012).

10 Busch, J. I. *et al.* Increased expression of the frontotemporal dementia risk factor TMEM106B causes C9orf72-dependent alterations in lysosomes. *Human molecular genetics* **25**, 2681-2697 (2016).

11 Butler, V. J. *et al.* Progranulin Stimulates the in vitro Maturation of pro-Cathepsin D at Acidic pH. *Journal of molecular biology* (2019).

12 Chang, M. C. *et al.* Progranulin deficiency causes impairment of autophagy and TDP-43 accumulation. *Journal of Experimental Medicine* **214**, 2611-2628 (2017).

13 Chen-Plotkin, A. S. *et al.* TMEM106B, the risk gene for frontotemporal dementia, is regulated by the microRNA-132/212 cluster and affects progranulin pathways. *Journal of Neuroscience* **32**, 11213-11227 (2012).

14 Cruts, M. *et al.* Null mutations in progranulin cause ubiquitin-positive frontotemporal dementia linked to chromosome 17q21. *Nature* **442**, 920 (2006).

15 Daniel, R., He, Z., Carmichael, K. P., Halper, J. & Bateman, A. Cellular localization of gene expression for progranulin. *Journal of Histochemistry & Cytochemistry* **48**, 999-1009 (2000).

16 Englund, B. *et al.* Clinical and neuropathological criteria for frontotemporal dementia. *J Neurol Neurosurg Psychiatry* **57**, 416-418 (1994).

17 Finch, N. *et al.* TMEM106B regulates progranulin levels and the penetrance of FTLD in GRN mutation carriers. *Neurology* **76**, 467-474 (2011).

18 Gass, J. *et al.* Mutations in progranulin are a major cause of ubiquitin-positive frontotemporal lobar degeneration. *Human molecular genetics* **15**, 2988-3001 (2006).

19 Götzl, J. K. *et al.* Common pathobiochemical hallmarks of progranulin-associated frontotemporal lobar degeneration and neuronal ceroid lipofuscinosis. *Acta neuropathologica* **127**, 845-860 (2014).

20 He, Z. & Bateman, A. Progranulin gene expression regulates epithelial cell growth and promotes tumor growth in vivo. *Cancer research* **59**, 3222-3229 (1999).

21 He, Z. & Bateman, A. Progranulin (granulin-epithelin precursor, PC-cell-derived growth factor, acrogranin) mediates tissue repair and tumorigenesis. *Journal of molecular medicine* **81**, 600-612 (2003).

22 He, Z., Ismail, A., Kriazhev, L., Sadvakassova, G. & Bateman, A. Progranulin (PC-cell-derived growth factor/acrogranin) regulates invasion and cell survival. *Cancer research* **62**, 5590-5596 (2002).

23 He, Z., Ong, C. H., Halper, J. & Bateman, A. Progranulin is a mediator of the wound response. *Nature medicine* **9**, 225 (2003).

24 Holler, C. J., Taylor, G., Deng, Q. & Kukar, T. Intracellular proteolysis of progranulin generates stable, lysosomal granulins that are haploinsufficient in patients with frontotemporal dementia caused by GRN mutations. *Eneuro* **4** (2017).

25 Hrabal, R., Chen, Z., James, S., Bennett, H. & Ni, F. The hairpin stack fold, a novel protein architecture for a new family of protein growth factors. *Nature structural biology* **3**, 747-752 (1996).

26 Hu, F. *et al.* Sortilin-mediated endocytosis determines levels of the frontotemporal dementia protein, progranulin. *Neuron* **68**, 654-667 (2010).

27 Jian, J. *et al.* Progranulin recruits HSP70 to β-glucocerebrosidase and is therapeutic against Gaucher disease. *EBioMedicine* **13**, 212-224 (2016).

28 Kang, J., Lim, L. & Song, J. TMEM106B, a risk factor for FTLD and aging, has an intrinsically disordered cytoplasmic domain. *PloS one* **13**, e0205856 (2018).

29 Klein, Z. A. *et al.* Loss of TMEM106B ameliorates lysosomal and frontotemporal dementia-related phenotypes in progranulin-deficient mice. *Neuron* **95**, 281-296. e286 (2017).

30 Kohlschütter, A. & Schulz, A. Towards understanding the neuronal ceroid lipofuscinoses. *Brain and Development* **31**, 499-502 (2009).

31 Kundu, S. T. *et al.* TMEM106B drives lung cancer metastasis by inducing TFEB-dependent lysosome synthesis and secretion of cathepsins. *Nature communications* **9**, 2731 (2018).

32 Lang, C. M. *et al.* Membrane orientation and subcellular localization of transmembrane protein 106B (TMEM106B), a major risk factor for frontotemporal lobar degeneration. *Journal of Biological Chemistry* **287**, 19355-19365 (2012).

33 Lee, C. W. *et al.* The lysosomal protein cathepsin L is a progranulin protease. *Molecular neurodegeneration* **12**, 55 (2017).

34 Lim, H. Y. *et al.* Progranulin contributes to endogenous mechanisms of pain defense after nerve injury in mice. *Journal of cellular and molecular medicine* **16**, 708-721 (2012).

35 Lui, H. *et al.* Progranulin deficiency promotes circuit-specific synaptic pruning by microglia via complement activation. *Cell* **165**, 921-935 (2016).

36 Mackenzie, I. R. *et al.* The neuropathology of frontotemporal lobar degeneration caused by mutations in the progranulin gene. *Brain* **129**, 3081-3090 (2006).

37 Marques, A. R. & Saftig, P. Lysosomal storage disorders–challenges, concepts and avenues for therapy: beyond rare diseases. *J Cell Sci* **132**, jcs221739 (2019).

38 Medina, D. L. *et al.* Transcriptional activation of lysosomal exocytosis promotes cellular clearance. *Developmental cell* **21**, 421-430 (2011).

39 Mukherjee, O. *et al.* HDDD2 is a familial FTLD-U caused by a missense mutation in progranulin. *Ann Neurol* **60**, 314-322 (2006).

40 Naphade, S. B. *et al.* Progranulin expression is upregulated after spinal contusion in mice. *Acta neuropathologica* **119**, 123-133 (2010).

41 Neary, D. *et al.* Frontotemporal lobar degeneration: a consensus on clinical diagnostic criteria. *Neurology* **51**, 1546-1554 (1998).

42 Nguyen, A. D. *et al.* Progranulin in the hematopoietic compartment protects mice from atherosclerosis. *Atherosclerosis* **277**, 145-154 (2018).

43 Nicholson, A. M. *et al.* TMEM 106B p. T185S regulates TMEM 106B protein levels: implications for frontotemporal dementia. *Journal of neurochemistry* **126**, 781-791 (2013).

44 Oberle, C. *et al.* Lysosomal membrane permeabilization and cathepsin release is a Bax/Bak-dependent, amplifying event of apoptosis in fibroblasts and monocytes. *Cell death and differentiation* **17**, 1167 (2010).

45 Palfree, R. G., Bennett, H. P. & Bateman, A. The evolution of the secreted regulatory protein progranulin. *PloS one* **10**, e0133749 (2015).

46 Paushter, D. H., Du, H., Feng, T. & Hu, F. The lysosomal function of progranulin, a guardian against neurodegeneration. *Acta neuropathologica*, 1-17 (2018).

47 Platt, F. M., Boland, B. & van der Spoel, A. C. Lysosomal storage disorders: The cellular impact of lysosomal dysfunction. *J Cell Biol* **199**, 723-734 (2012).

48 Plowman, G. D. *et al.* The epithelin precursor encodes two proteins with opposing activities on epithelial cell growth. *Journal of Biological Chemistry* **267**, 13073-13078 (1992).

49 Pottier, C., Ravenscroft, T. A., Sanchez-Contreras, M. & Rademakers, R. Genetics of FTLD: overview and what else we can expect from genetic studies. *Journal of neurochemistry* **138**, 32-53 (2016).

50 Ratnavalli, E., Brayne, C., Dawson, K. & Hodges, J. The prevalence of frontotemporal dementia. *Neurology* **58**, 1615-1621 (2002).

51 Ryan, C. L. *et al.* Progranulin is expressed within motor neurons and promotes neuronal cell survival. *BMC neuroscience* **10**, 130 (2009).

52 Sanborn, K. B. *et al.* Myosin IIA associates with NK cell lytic granules to enable their interaction with F-actin and function at the immunological synapse. *The Journal of Immunology* **182**, 6969-6984 (2009).

53 Sardiello, M. *et al.* A gene network regulating lysosomal biogenesis and function. *Science* **325**, 473-477 (2009).

54 Schwenk, B. M. *et al.* The FTLD risk factor TMEM106B and MAP6 control dendritic trafficking of lysosomes. *The EMBO journal* **33**, 450-467 (2014).

55 Shoyab, M., McDonald, V. L., Byles, C., Todaro, G. J. & Plowman, G. D. Epithelins 1 and 2: isolation and characterization of two cysteine-rich growth-modulating proteins. *Proceedings of the National Academy of Sciences* **87**, 7912-7916 (1990).

56 Smith, K. R. *et al.* Strikingly different clinicopathological phenotypes determined by progranulin-mutation dosage. *The American Journal of Human Genetics* **90**, 1102-1107 (2012).

57 Songsrirote, K., Li, Z., Ashford, D., Bateman, A. & Thomas-Oates, J. Development and application of mass spectrometric methods for the analysis of progranulin N-glycosylation. *Journal of proteomics* **73**, 1479-1490 (2010).

58 Stagi, M., Klein, Z. A., Gould, T. J., Bewersdorf, J. & Strittmatter, S. M. Lysosome size, motility and stress response regulated by fronto-temporal dementia modifier TMEM106B. *Molecular and Cellular Neuroscience* **61**, 226-240 (2014).

59 Tanaka, Y., Chambers, J. K., Matsuwaki, T., Yamanouchi, K. & Nishihara, M. Possible involvement of lysosomal dysfunction in pathological changes of the brain in aged progranulin-deficient mice. *Acta neuropathologica communications* **2**, 78 (2014).

60 Tolkatchev, D. *et al.* Structure dissection of human progranulin identifies well-folded granulin/epithelin modules with unique functional activities. *Protein Science* **17**, 711-724 (2008).

61 Tolkatchev, D., Ng, A., Vranken, W. & Ni, F. Design and solution structure of a well-folded stack of two β-hairpins based on the amino-terminal fragment of human granulin A. *Biochemistry* **39**, 2878-2886 (2000).

62 Valdez, C. *et al.* Progranulin-mediated deficiency of cathepsin D results in FTD and NCL-like phenotypes in neurons derived from FTD patients. *Human molecular genetics* **26**, 4861-4872 (2017).

63 Van Blitterswijk, M. *et al.* TMEM106B protects C9ORF72 expansion carriers against frontotemporal dementia. *Acta neuropathologica* **127**, 397-406 (2014).

64 Van Deerlin, V. M. *et al.* Common variants at 7p21 are associated with frontotemporal lobar degeneration with TDP-43 inclusions. *Nature genetics* **42**, 234 (2010).

65 Vancha, A. R. *et al.* Use of polyethyleneimine polymer in cell culture as attachment factor and lipofection enhancer. *BMC biotechnology* **4**, 23 (2004).

66 Vass, R. *et al.* Risk genotypes at TMEM106B are associated with cognitive impairment in amyotrophic lateral sclerosis. *Acta neuropathologica* **121**, 373-380 (2011).

67 Vranken, W. *et al.* A 30-residue fragment of the carp granulin-1 protein folds into a stack of two β-hairpins similar to that found in the native protein. *The Journal of peptide research* **53**, 590-597 (1999).

68 Ward, M. E. *et al.* Individuals with progranulin haploinsufficiency exhibit features of neuronal ceroid lipofuscinosis. *Science translational medicine* **9**, eaah5642 (2017).

69 Whitwell, J. L., Jack, C. R., Senjem, M. L. & Josephs, K. A. Patterns of atrophy in pathologically confirmed FTLD with and without motor neuron degeneration. *Neurology* **66**, 102-104 (2006).

70 Wils, H. *et al.* Cellular ageing, increased mortality and FTLD-TDP-associated neuropathology in progranulin knockout mice. *The Journal of pathology* **228**, 67-76 (2012).

71 Yin, F. *et al.* Exaggerated inflammation, impaired host defense, and neuropathology in progranulin-deficient mice. *Journal of Experimental Medicine* **207**, 117-128 (2010).

72 Yin, F. *et al.* Behavioral deficits and progressive neuropathology in progranulin-deficient mice: a mouse model of frontotemporal dementia. *The FASEB Journal* **24**, 4639-4647 (2010).

73 Zheng, Y., Brady, O. A., Meng, P. S., Mao, Y. & Hu, F. C-terminus of progranulin interacts with the beta-propeller region of sortilin to regulate progranulin trafficking. *PloS one* **6**, e21023 (2011).

74 Zhou, X. *et al.* Lysosomal processing of progranulin. *Molecular neurodegeneration* **12**, 62 (2017).

75 Zhou, X., Sullivan, P. M., Sun, L. & Hu, F. The interaction between progranulin and prosaposin is mediated by granulins and the linker region between saposin B and C. *Journal of neurochemistry* **143**, 236-243 (2017).

76 Zhou, X. *et al.* Impaired prosaposin lysosomal trafficking in frontotemporal lobar degeneration due to progranulin mutations. *Nature communications* **8**, 15277 (2017).

77 Zhou, X. *et al.* Prosaposin facilitates sortilin-independent lysosomal trafficking of progranulin. *J Cell Biol* **210**, 991-1002 (2015).